

Coherent Diabatic Ion Transport and Separation in a Multi-Zone Trap Array

R. Bowler,* J. Gaebler, Y. Lin, T. R. Tan, D. Hanneke,† J. D. Jost, J. P. Home,‡ D. Leibfried, and D. J. Wineland

We investigate the motional dynamics of single and multiple ions during transport between and separation into spatially distinct locations in a multi-zone linear Paul trap. A single ${}^9\text{Be}^+$ ion in a ~ 2 MHz harmonic well located in one zone was laser-cooled to near its ground state of motion and transported $370\ \mu\text{m}$ by moving the well to another zone. This was accomplished in $8\ \mu\text{s}$, corresponding to 16 periods of oscillation. Starting from a state with $\bar{n} \approx 0.1$ quanta, during transport the ion was excited to a displaced coherent state with $\bar{n} \approx 1.6$ quanta but on completion was returned close to its motional ground state with $\bar{n} \approx 0.2$. Similar results were achieved for the transport of two ions. We also separated chains of up to 9 ions from one potential well to two distinct potential wells. With two ions this was accomplished in $55\ \mu\text{s}$, with final excitations of $\bar{n} \approx 2$ quanta for each ion. Fast coherent transport and separation can significantly reduce the time overhead in certain architectures for scalable quantum information processing with trapped ions.

For quantum information processing (QIP) based on trapped ions [1], scaling might be achieved with an array of interconnected trap zones where information transport is accomplished by confining the ions in potential wells that are moved between zones [2, 3]. The basic features of this scheme have been demonstrated in the situation where ion qubits were transported adiabatically, on a time scale much greater than the period corresponding to the ions' oscillation frequencies in their local wells. This suppresses undesired motional excitation that can impede the ability to perform high-fidelity multi-qubit quantum logic gates [4–8]. In [9], one and two ions were separated from a group of three in 2 ms with mode excitation less than one quantum. In [5–7] a mixed-ion linear chain or “crystal” of ions was separated into two ${}^9\text{Be}^+ \cdot {}^{24}\text{Mg}^+$ pairs accompanied by motional excitation that could be removed with sympathetic laser cooling. In these latter experiments, the time required for ion separation, transport, and sympathetic laser cooling was 100 times larger than for logic gates (approximately 5 and $20\ \mu\text{s}$ for single and two-qubit gates, respectively), emphasizing the potential for improvement.

With the goal of reducing the time required for ion separation, transport, and sympathetic laser cooling, we have investigated diabatic transport and separation. In [10], diabatic ion transport was accomplished on a time scale corresponding to four oscillation periods, but this resulted in large motional excitation. Diabatic transport with small final excitation of the center-of-mass (COM) motion has been observed for cold neutral-atom ensembles on 1 s timescales (on the order of a single oscillation period) [11]. Here we demonstrate diabatic ion transport in a duration ($8\ \mu\text{s}$) comparable to that for gate operations, with significantly suppressed final excitation. We also demonstrate the separation of two ${}^9\text{Be}^+$ ions from a common harmonic well into spatially distinct wells in

$55\ \mu\text{s}$ and with a final excitation of approximately two quanta.

Transport and separation of ions can be implemented by applying time-varying potentials (waveforms) to segmented trap electrodes. In the experiments described here, ions are confined in a multi-zone linear Paul trap (Fig. 1) in which an ion's local potential well can be made harmonic to a good approximation. To determine the total potential at any given time in a waveform, we use simulations of potentials from individual electrodes that are linearly superposed. Along the trap axis (horizontal in Fig. 1), the confinement is characterized by (angular) frequency ω . Confinement in the transverse direction is significantly stronger and does not play a significant role here. The custom-built waveform electronics have an update rate of 50 MHz, far above axial mode frequencies, enabling considerable changes in potential within single periods of oscillation. Zones A, X, and B are regions near the respective electrodes through which ions travel along the trap axis, while the outer electrodes O1 and O2 are used only for potential optimization.

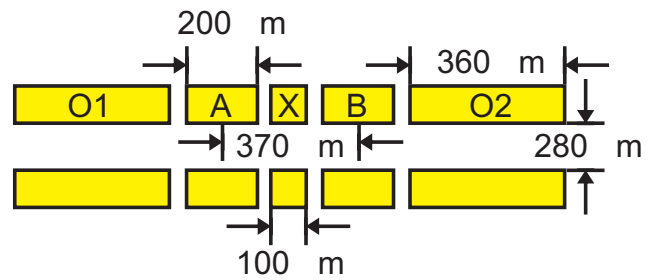


FIG. 1. Schematic of the linear Paul (quadrupole) ion trap electrode structure showing the two diagonally opposite segmented DC electrodes (not to scale; trap details in [5–7, 12]). Ions are loaded in a region to the left of electrode O1 and initially transported to zone A. Trap radio-frequency (RF) electrodes (not shown) are referenced to a common ground potential.

The qubit is formed from two $2s^2S_{1/2}$ electronic ground-state hyperfine levels of ${}^9\text{Be}^+$ $|F = 2, m_F = 1\rangle \equiv$

* ryan.bowler@nist.gov

† Current address: Department of Physics, Amherst College, Amherst, MA, 01002-5000 USA

‡ Current address: Institute for Quantum Electronics, ETH Zurich, 8093 Zurich, CH

$|\downarrow\rangle$ and $|F=1, m_F=0\rangle \equiv |\uparrow\rangle$, separated in frequency by $\omega_0/(2\pi) \simeq 1.2$ GHz, where F and m_F are the ion's total angular momentum and its projection along the quantizing magnetic field ($\simeq 11.9$ mT). Ion motional quantum states can be described in the Fock state basis $|n\rangle$ with energy $\hbar\omega(n + \frac{1}{2})$. To characterize the motional states experimentally, we use two laser beams detuned from each other by $\omega_0 + \omega$ or $\omega_0 - \omega$ to drive motion adding sideband (MAS) spin-flip transitions $|\downarrow, n\rangle \rightarrow |\uparrow, n+1\rangle$ or motion subtracting sideband (MSS) transitions $|\downarrow, n\rangle \rightarrow |\uparrow, n-1\rangle$, respectively, via stimulated-Raman transitions. Acousto-optic deflectors enable the laser beams to be directed to either zone A or B. Since the corresponding Rabi rates $\Omega_{n, n\pm 1}$ are n -dependent, the populations P_n of Fock states can be determined from the probability $P_\downarrow(t)$ of the state $|\downarrow\rangle$ as a function of drive time t , derived from state-dependent resonance fluorescence [13]. As an approximation, we fit to the function $P_\downarrow(t) = \frac{1}{2}(1 + e^{-\gamma t} \sum_{n=0} P_n \cos(2\Omega_{n, n\pm 1} t))$ to include a phenomenological decay rate γ .

Theoretical investigations of optimal transport of atomic systems involve analyzing the acceleration and deceleration of an ion in a way to minimize excitation of motion for a given transport duration. [10, 14–17]. In our experiments, the transport waveforms are designed to move the ions in a constant-curvature harmonic potential characterized by ω ; if the ion starts in the ground state, its quantum-mechanical motion will be a displaced coherent state that follows a classical trajectory [18]. A coherent state in such a well is characterized by a complex amplitude α where $|\alpha|^2 = \bar{n}$. For transport along z we can write the potential as $\frac{1}{2}m\omega^2(z - z_0(t))^2$, where m is the mass of the ion and $z_0(t)$ is the minimum of the well. In [17], it has been shown that the coherent state displacement $\alpha(t)$ resulting from transport in the frame of the well center is

$$\alpha(t) = \sqrt{\frac{m\omega}{2\hbar}} \left(-e^{-i\omega t} \int_0^t \dot{z}_0(t') e^{i\omega t'} dt' \right). \quad (1)$$

As long as the Fourier component of $\dot{z}_0(t')$ at the trap frequency vanishes when integrated over the transport duration, the ion will end up in its initial state at position $z_0(t)$. A simple case where the well impulsively starts moving at constant velocity v and then stops at time t_T ($\dot{z}_0 = 0$ for $t < 0$ and $t > t_T$, and $\dot{z}_0 = v$ for $t \in [0, t_T]$) leads to

$$\alpha(t_T) = \sqrt{\frac{m\omega}{2\hbar}} \left(i \frac{v}{\omega} [1 - e^{-i\omega t_T}] \right). \quad (2)$$

For $\omega t_T = 2\pi N$, with N an integer, an ion starting in its ground state of motion is caught back in the ground state, as in [11]. For non-integer N , the ion will be left in a coherent state different from the ground state. Due to the finite response times of our electrode drive electronics, sudden starts and stops are not practical. Nevertheless, Eq.(1) gives a criterion for transport functions $z_0(t)$

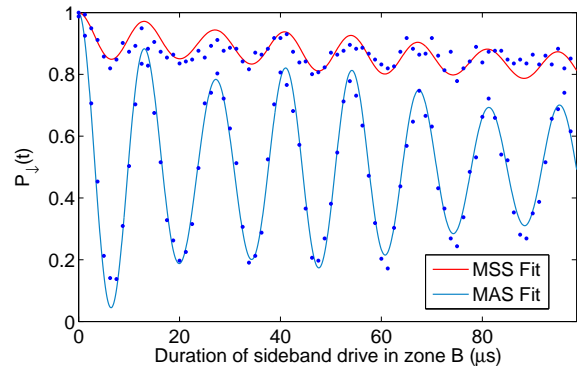


FIG. 2. Rabi flopping trace on the MAS and MSS after transport from zone A to B. Here we fit to thermal distributions that give $\bar{n} = 0.19 \pm 0.02$ from the MAS fit and $\bar{n} = 0.17 \pm 0.01$ from the MSS fit. The axial frequency was $\omega/(2\pi) = 1.972(1)$ MHz with a Lamb-Dicke parameter $\eta = 0.479$.

that leave the ion in the ground state after the transport is completed. More generally, one can always find a coherent displacement that returns the ion to its ground state.

As a demonstration of diabatic transport, a single ion in zone A ($\omega/(2\pi) \simeq 2$ MHz; $\{V_{O1}, V_A, V_X, V_B, V_{O2}\} = \{1.289, 0.327, 2.173, 0.310, 1.311\}$ V) was first initialized; it was laser-cooled to a thermal distribution with $\bar{n} \approx 0.1$ and optically pumped to $|\downarrow\rangle$. It was then transported $370 \mu\text{m}$ in $t_T \approx 8 \mu\text{s}$ to zone B (A \rightarrow B). Following transport, qubit sideband transitions were driven in zone B, then the ion was transported back to zone A (B \rightarrow A) to determine $P_\downarrow(t)$. By varying ω , we minimized the final excitation for $\omega/(2\pi) = 1.972(1)$ MHz corresponding approximately to $N = 16$ (Fig. 2). Excitation was also minimized for values of $\omega/2\pi$ differing from this value by integer multiples of t_T^{-1} .

For other values of $\omega/(2\pi)$, $P_\downarrow(t)$ measurements showed that the final motional states were consistent with coherent state probability distributions over Fock states; however, these measurements do not verify the coherences between Fock states. To verify that the transport excites a coherent state, we implemented A \rightarrow B transport in a well of frequency $\omega/(2\pi) = 1.919(2)$ MHz such that $\alpha(t_T) \neq 0$ in zone B (Fig.3). We then applied a uniform electric field $E_z = E_0 \cos(\omega t_E + \phi_E)$ to provide a phase-space displacement α_E . This was followed by a sideband drive of duration t , transport back to zone A, and measurement of $P_\downarrow(t)$. By adjusting E_0 , t_E , and ϕ_E (relative to the time when transport started), we could make $\alpha_E = -\alpha(t_T)$. Under these conditions, we measured a final state at $\bar{n} = 0.19 \pm 0.02$. In addition, when $\alpha(t_T) \neq 0$ in zone B, by waiting an appropriate delay $T_d \pm N2\pi/\omega$ in B, and then transporting back to zone A, the ion would be returned to its ground state in A (A \rightarrow B \rightarrow A “cold” transport).

Internal state qubit coherences are reliably maintained during transport [4, 8]. Under transport with minimal fi-

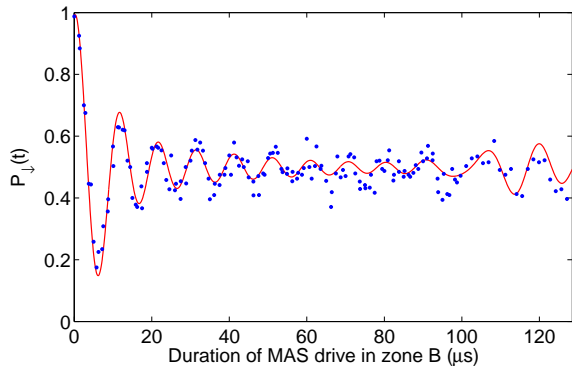


FIG. 3. Rabi flopping trace on the MAS following transport in which $\alpha(t_T) \neq 0$. The figure shows a coherent state fit with $\bar{n} = 6.4 \pm 0.2$, corresponding to $|\alpha| = 2.53 \pm 0.04$. The axial frequency was $\omega/(2\pi) = 1.919(2)$ MHz and the Lamb-Dicke parameter was $\eta = 0.486$.

nal excitation we can expect that since any Fock state receives the same phase-space displacement across the transport, initial motional states should maintain the same relative coherences before and after transport. To demonstrate this, we performed a Ramsey-type interference experiment. After state initialization, a MAS $\pi/2$ pulse was applied to transform the state to $\frac{1}{\sqrt{2}}(|\downarrow, n=0\rangle + |\uparrow, n=1\rangle)$. To establish a baseline reference, we first waited for a time equal to the duration for $A \rightarrow B \rightarrow A$ cold transport followed by a second MAS $\pi/2$ pulse of variable phase. In this case we measured a fringe contrast of 85(2) %, limited primarily by imperfect initial ground-state cooling and the relatively large Lamb-Dicke parameter. When we performed the experiment with $A \rightarrow B \rightarrow A$ cold transport between Ramsey pulses, the measured 86(2) % contrast was consistent with no loss in coherence.

We also transported two ${}^9\text{Be}^+$ ions ($A \rightarrow B$) in the same well. If the moving potential well is maintained at constant frequency, the “stretch” mode (ion motion out-of-phase) should not be excited and the the COM mode should be excited as for a single ion. We initialized both modes to $\bar{n} \approx 0.1$ and after transport observed $\bar{n}_{COM} = 0.35 \pm 0.1$, with negligible excitation of the stretch mode.

When separating multiple ions confined in a single well into two separate wells, it is impossible to preserve the motional mode frequencies. To lowest order, the required external potential can be described as the sum of a quadratic and a quartic term for $0 \leq t \leq t_s$ during separation [19]:

$$U(z) = a(t)z^2 + b(t)z^4, \quad (3)$$

with $a(0) > 0$, $b(0) = 0$ and $a(t_s) < 0$, $b(t_s) > 0$. Due to Coulomb repulsion, the normal modes of multiple ions remain harmonic throughout the separation for small excursions about each ion’s local minimum. The normal-mode frequencies go through their minima near the point

when a vanishes and the quartic potential dominates the confinement.

Our waveform for separation was divided into two main segments. Ions were first transported to zone X, whose center is defined as $z = 0$ relative to Eq.(3). Then $a(t)$ was decreased and $b(t)$ increased by lowering the potentials on electrodes A and B while simultaneously increasing the potentials on outer electrodes O1 and O2 until the mode frequencies approximately reach their minimum values. In the second segment, we separated the ions into distinct wells in zones A and B by increasing the potential on electrode X such that $a(t)$ changed sign, creating a “wedge” that splits the ions apart.

As one demonstration of ion separation control, we ran a separation waveform (duration $\approx 340 \mu\text{s}$) to partition a linear crystal of nine ${}^9\text{Be}^+$ ions into all possible combinations. We first Doppler cooled the crystal in zone A and optically pumped to $|\downarrow_1, \downarrow_2, \dots, \downarrow_9\rangle$. It was then transported it to zone X for separation into two groups in zones A and B. A variable offset potential V_{O2} applied to electrode O2 imposed an electric field in zone X that shifted the center of the crystal relative to the separation wedge and determined the number of ions in each group. Ions in zone A were detected with laser-induced fluorescence, approximately proportional to ion number. Following detection, all ions were recombined and transported to zone A where the number was checked. As shown in Fig.4, increasing V_{O2} led to increased ion numbers in zone A. By adjusting V_{O2} to the center of a certain step, we could reliably partition the ions into two groups of predetermined number.

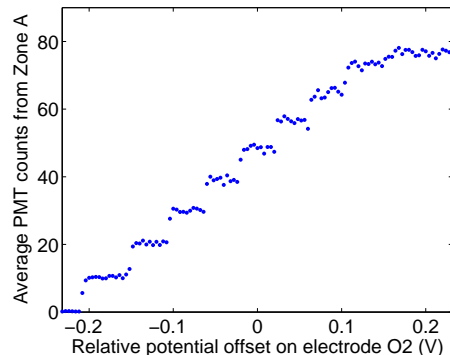


FIG. 4. Ion fluorescence in zone A as a function of the offset potential on electrode O2 during separation relative to a central value. Each step increase of the fluorescence corresponds to the presence of an additional ion in zone A after separation. Any number of the nine ions could be reliably separated into zone A by setting the offset potential to the center of the respective step. Fluorescence of a single ion led to approximately 10 average photomultiplier tube (PMT) counts in the detection period, but as more ions were added in zone A, the crystal was no longer uniformly illuminated by the detection beam and the total fluorescence dropped below 10 counts per ion.

During separation, diabatic changes in both curvature

and minimum position of the axial potential can lead to coherent displacement and squeezing of the motional states. The change in ω as well as the accelerations of the potential well minima are both determined by the rate of change in the separating wedge. The largest excitation during separation coincides with the least adiabatic changes in mode frequencies, near the time when the quadratic component of the potential changes sign [19]. These excitations can be suppressed by approximating the adiabatic condition for ramping a harmonic well, $\frac{1}{\omega^2} \frac{d\omega}{dt} \ll 1$ [20]. We numerically solved for this quantity in our waveform and imposed a maximum value of $\frac{1}{\omega^2} \frac{d\omega}{dt} = 0.025$ for the COM mode during the ramp-down of the harmonic well and $\frac{1}{\omega^2} \frac{d\omega}{dt} = 0.015$ around the sign change of a in Eq.(3).

A two-ion crystal in zone X with an initial well frequency of $\omega/(2\pi) = 2.6$ MHz ($\{V_{O1}, V_A, V_X, V_B, V_{O2}\} = \{2.433, -0.3763, -1.7089, -0.3831, 2.473\}$ V) could be separated and one ion placed in zones A and B (with motional frequencies 2.85 MHz and 2.77 MHz respectively, $\{V_{O1}, \dots, V_{O2}\} = \{4.441, -5.252, -0.649, -5.411, 5.952\}$ V) in a duration of 55 μ s. After separation, qubit MAS transitions of varying duration t were driven on either the ion in zone A or B followed by recombination in zone A, whereupon fluorescence state detection was performed to determine $P_{\downarrow}(t)$ for each ion. The first separation segment took 17 μ s, during which it was necessary to ramp V_{O2} from 2.473 to 5.952 V to compensate for trap geometric asymmetries and to center the crystal over the separation wedge; the final value was set by minimizing \bar{n} for both ions. Near the point of ion separation, simulation predicted that the minimum COM mode frequency was 880 kHz and minimum stretch mode frequency was 700 kHz. During the second separation segment we obtained best results by also applying a variable offset potential to electrode X to tune the quartic component $b(t)$ in the potential. We also applied a relative difference between electrodes A and B to compensate for trap imperfections and make the potential well as symmetric as possible about electrode X. This enabled a fine-tune balancing of the final excitation between the two ions. Experimentally, we found that equal excitation in both final zones gave the lowest total excitation to both ions.

The two-ion crystal was initialized in zone X to a thermal state with $\bar{n} \approx 0.1$ on both the COM and stretch modes and optical pumping to $|\downarrow_1 \downarrow_2\rangle$. After separation, sideband excitation gave Fock state populations consistent with coherent states of $\bar{n} = 2.1 \pm 0.1$ in zone A and $\bar{n} = 1.9 \pm 0.1$ in zone B (Fig.5). With RF de-excitation of each ion, we could reduce \bar{n} to 1.4 ± 0.1 and 1.6 ± 0.1 in zones A and B respectively, consistent with a thermal distribution. The reductions indicated partial coherence of the final states. The residual excitations could not be explained by ambient heating; we measured the heating rates of a single ion over the range of mode frequencies experienced by the ions during separation and determined that the integrated heating rates would lead to an additional $\Delta\bar{n} \approx 0.2$. The fact that we couldn't

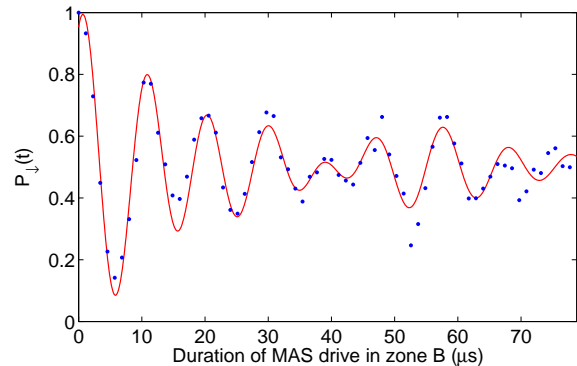


FIG. 5. Rabi flopping trace of the MAS of the ion in zone B after separation. The fits are to a coherent state with $\bar{n} = 1.9 \pm 0.1$, and $|\alpha| = 1.38 \pm 0.04$ ($\eta = 0.404$). The trace for the ion in zone A looks very similar giving $\bar{n} = 2.1 \pm 0.1$, or $|\alpha| = 1.45 \pm 0.03$ ($\eta = 0.399$).

reduce \bar{n} further could be explained if the phase of the coherent states changed significantly from experiment to experiment. This seems plausible, given the sensitivity of the ions' local wells to slight changes in electrode potentials at the point when the local potential curvatures are near their minima. As an example, for a change of V_{O2} of +3 mV, the motion of the ion in zone A had $\bar{n} \approx 1.14 \pm 0.07$, while the ion in zone B had $\bar{n} > 15$, which then could be coherently de-excited to a state consistent with a thermal distribution having $\bar{n} = 3.8 \pm 0.5$. The large excitation of the ion in B can be qualitatively explained; since it is closer to the maximum of the wedge during separation, it would be expected to gain more kinetic energy as it accelerates towards the center of its respective well.

In summary, we have demonstrated diabatic transport of one and two ions and separation of two ions in a multi-zone linear trap on 10 μ s time scales, which approach those of logic gate operations. When transporting and separating ions on a time scale that approached the ions' local well oscillation periods, we observed coherent excitation of the motion that could be avoided by shaping the waveform appropriately or nearly eliminated by a coherent displacement that was applied after transport or separation. In addition, multi-ion crystals were reliably partitioned into two groups of predetermined numbers. These methods can reduce the time overhead for separation, transport, and re-cooling in scalable implementations of large quantum information algorithms.

The spatial extent of the separating "wedge" is governed by the ion-to-electrode distances; therefore, smaller traps can accomplish fast separation while maintaining stronger confinement, which would lead to reduced excitation if background motional heating can be suppressed. In principle it should be possible to transport like ions between two zones in arbitrarily short durations [21]; however, when potential curvatures at the ion positions are time-dependent, squeezing must also be taken into

account for both transport and separation (In the experiments reported here, squeezing was estimated to be negligible). Moreover, experiments that use a different species for sympathetic laser cooling [5–7] will require special consideration since all modes will be excited during both diabatic transport and separation.

This work is supported by IARPA, NSA, ONR, DARPA & the NIST Quantum Information Program. We thank J. Heidecker for electronics support and D. Slichter and A. Wilson for helpful comments on the manuscript. Contribution of NIST; not subject to U.S. copyright.

-
- [1] J. I. Cirac and P. Zoller, *Phys. Rev. Lett.* **74**, 4091 (1995).
 [2] D. J. Wineland *et al.*, *J. Res. Natl. Inst. Stand. Technol.* **103**, 259 (1998).
 [3] D. Kielpinski, C. Monroe, and D. Wineland, *Nature* **417**, 709 (2002).
 [4] M. A. Rowe *et al.*, *Quantum Information and Computation* **2**, 257 (2002).
 [5] J. D. Jost *et al.*, *Nature (London)* **459**, 683 (2009).
 [6] J. P. Home *et al.*, *Science* **325**, 1227 (2009).
 [7] D. Hanneke *et al.*, *Nature Physics* **6**, 13 (2010).
 [8] R. B. Blakestad *et al.*, *Phys. Rev. A* **84**, 032314 (2011).
 [9] M. D. Barrett *et al.*, *Nature* **429**, 737 (2004).
 [10] G. Huber *et al.*, *New J. Phys.* **10**, 013004 (2008).
 [11] A. Couvert, T. Kawalec, G. Reinaudi, and D. Guery-Odelin, *Europhys. Lett.* **83**, 13001 (2008).
 [12] J. Jost, Ph.D. thesis, Department of Physics, University of Colorado, Boulder, 2010.
 [13] D. M. Meekhof *et al.*, *Phys. Rev. Lett.* **76**, 1796 (1996), erratum *Phys. Rev. Lett.* **77**, 2346 (1996).
 [14] R. Reichle *et al.*, *Fortschr. Phys.* **54**, 666 (2006).
 [15] S. Schulz, U. Poschinger, K. Singer, and F. Schmidt-Kaler, *Fortschr. Phys.* **54**, 648 (2006).
 [16] E. Torrontegui *et al.*, *Phys. Rev. A* **83**, 013415 (2011).
 [17] H.-K. Lau and D. F. V. James, *Phys. Rev. A* **83**, 062330 (2011).
 [18] D. Leibfried, R. Blatt, C. Monroe, and D. Wineland, *Rev. Modern Phys.* **75**, 281 (2003).
 [19] J. P. Home and A. M. Steane, *Quantum Information and Computation* **6**, 289 (2006).
 [20] X. Chen *et al.*, *Phys. Rev. Lett.* **104**, 063002 (2010).
 [21] D. J. Wineland, *Int. School of Physics Enrico Fermi*, F. De Martini and C. Monroe, eds., IOS Press, Amsterdam **148**, 165 (2002).